

ORIGINAL ARTICLE

Biological evaluation and determination of the absolute configuration of chloromonilicin, a strong antimicrobial metabolite isolated from *Alternaria sonchi*

Alessio Cimmino¹, Gennaro Pescitelli², Alexander Berestetskiy³, Anna Dalinova³, Denis Krivorotov⁴, Angela Tuzi¹ and Antonio Evidente¹

Chloromonilicin was isolated for the first time from *Alternaria sonchi*, a mycoherbicide proposed for the control of the noxious weed *Sonchus arvensis*. The already known alternethanoxins A and B and the three recently isolated phytotoxic polycyclic ethanones named alternethanoxins C–E were also isolated from the same source. Chloromonilicin was identified by spectroscopic data (essentially one-dimensional NMR, 2-dimensional NMR and high-resolution ESI-MS) and its structure was confirmed by single X-ray analysis, which also allowed the assignment of the absolute configuration. This latter was independently confirmed by electronic CD calculations. When chloromonilicin was tested for its antimicrobial activity, it was active at concentrations 0.5–1 µg per disc against four bacterial species and a yeast fungus. The compound inhibited conidial germination of four plant pathogens at concentration of 1–10 µg ml⁻¹. No phytotoxic activity of this antibiotic by leaf-disc puncture bioassay was detected. *The Journal of Antibiotics* (2016) 69, 9–14; doi:10.1038/ja.2015.74; published online 15 July 2015

INTRODUCTION

Sonchus arvensis L., commonly called perennial sow thistle, is considered to be an important weed in Europe and North America. It infests many habitats such as cultivated fields, roadsides, pastures and lawns with consequent heavy economic losses. Most of the herbicides recommended for the control of *S. arvensis* are generally restricted to only a few active ingredients that tend to have low selectivity, especially for dicots crops.¹ Natural enemies of weeds such as plant pathogens could be used for weed biocontrol as an eco-friendly and quite selective support of crop protection measures.² Two plant pathogenic fungi, *Alternaria sonchi* J.J. Davis and *Phoma exigua* Desm. var. *exigua* have been considered as potential mycoherbicides for *S. arvensis*.³

It is well known that plant pathogens such as fungi and bacteria produce numerous secondary metabolites including virulence and defense factors. Phytotoxins can be used as natural herbicides or models for the synthesis of herbicidal biorationals. Metabolites with different types of biological activity may have positive or negative side effects on macroorganisms and soil microflora.⁴ For this reason, the chemistry of weed biocontrol agents should be studied as deeply as possible. For example, *Ph. exigua* var. *exigua* was found to produce numerous cytotoxic cytochalasins. The presence of these compounds could be a restriction for a practical application of the fungus as a bioherbicide.⁵

Extracts of *A. sonchi* obtained from solid cultures of the fungus were shown to have a phytotoxic and an antimicrobial activity.⁶ Five polycyclic ethanones (phytotoxins and weak antimicrobials), namely, alternethanoxins A–E were isolated from the fungal solid culture.^{7,8} Alternethanoxins A and B, as well as the dimethyl derivative of alternethanoxin A, showed cytostatic growth inhibitory effect when evaluated on six cell lines for their anticancer activity.⁹ These studies demonstrated that *A. sonchi* is a rich source of new and interesting metabolites.

Further investigation of the organic extract of *A. sonchi* solid culture allowed the isolation of a known but poorly characterized antimicrobial metabolite belonging to xanthone group. This manuscript reports the isolation of chloromonilicin (**1**, Figure 1) from the solid culture of *A. sonchi* as the first finding of this metabolite in *Alternaria* fungi. Chloromonilicin, which represents the main fungal metabolite, appeared to be non-phytotoxic but showed a strong antimicrobial activity. The potential of *A. sonchi* as a mycoherbicide and its environmental safety is discussed.

MATERIALS AND METHODS

Chemistry

Melting points were measured on an Axioskop Zeiss microscope (Zeiss, Jena, Germany) coupled with a Mettler FP90 hot (Mettler, Greifensee, Switzerland); optical rotation was measured on a Jasco P-1010 digital polarimeter (JASCO, Tokyo, Japan); and electronic CD (ECD) spectra were recorded on a JASCO

¹Dipartimento di Scienze Chimiche, Università di Napoli Federico II, Complesso Universitario Monte S. Angelo, Napoli, Italy; ²Dipartimento di Chimica e Chimica Industriale, Università di Pisa, Pisa, Italy; ³Department of Phytotoxicology and Biotechnology, All-Russian Institute of Plant Protection, Federal Agency of Scientific Organizations, Pushkin, Saint Petersburg, Russian Federation and ⁴Department of Chemical Modelling, Research Institute of Hygiene, Occupational Pathology and Human Ecology, Federal Medical Biological Agency, Saint-Petersburg, Russian Federation

Correspondence: Professor A Evidente, Dipartimento di Scienze Chimiche, Università di Napoli Federico II, Complesso Universitario Monte S. Angelo, Via Cintia 4, Napoli 80126, Italy. E-mail: evidente@unina.it

Received 24 November 2014; revised 3 March 2015; accepted 8 June 2015; published online 15 July 2015

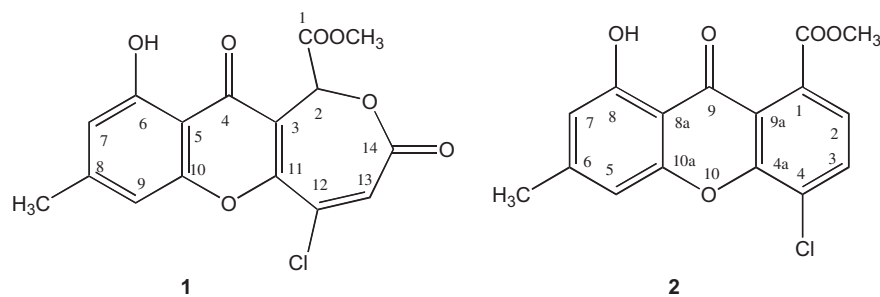


Figure 1 Structures of chloromonilicin (**1**) and its biosynthetic precursor 4-chloropsin (**2**).

Table 1 ^1H (400 MHz), ^{13}C NMR (100 MHz) and HMBC data of chloromonilicin in CD_3COCD_3 (**1**)^{a,b}

Position	$\delta_{\text{C}}^{\text{c}}$ (m)	δ_{H} (m, J)	HMBC
1	169.2 (s)		OMe
2	68.7 (d)	6.48 (1H, s)	OMe
3	120.4 (s)		
4	181.2 (s)		H-9, H-7, H-2
5	109.8 (s)		H-9, H-7
6	158.3 (s)		
7	110.1 (d)	7.02 (1H, s ^d)	H-9, C-CH ₃
8	152.0 (s)		
9	115.3 (d)	6.81 (1H, s ^d)	H-7, C-CH ₃
10	162.4 (s) ^e		
11	162.1 (s) ^e		H-2
12	136.4 (s)		H-13
13	132.0 (d)	7.16 (1H, s)	
14	163.5 (s)		
C-CH ₃	23.6 (q)	2.29 (3H, s ^d)	
O-CH ₃	55.2 (q)	3.83 (3H, s)	
OH		11.82 (1H, s)	

^aChemical shifts are in δ values (p.p.m.) from TMS.

^b2D ^1H , ^1H (COSY) and ^{13}C , ^1H (HMQC) NMR experiments confirmed the correlations of all the protons and the corresponding carbons.

^cMultiplicities were assigned with DEPT.

^dThe protons H-7 and H-9 were themselves and both coupled with C-CH₃ probably with $J < 1$ Hz.

^eThese two carbons are previously reported as an overlapped signal.⁶

J-815 spectropolarimeter in acetonitrile. IR spectrum was recorded as deposit glass film on a Thermo Electron Corporation Nicolet 5700 FT-IR spectrometer (Thermo Scientific, WI, USA) and UV spectra were measured in MeOH and acetonitrile on a Jasco V-530 spectrophotometer. ^1H and ^{13}C NMR spectra were recorded at 400 and 100 MHz, respectively, in CD_3COCD_3 on a Bruker AVANCE III 400 MHz spectrometer (BRUKER, Karlsruhe, Germany). The same solvent was used as internal standard. COSY-45, HMQC, HMBC and ROESY experiments¹⁰ were performed using standard Bruker pulse sequences. High-resolution (HR) ESI-MS spectra were recorded on Agilent 6530 Q-TOF LC/MS spectrometer (Agilent, Moscow, Russia). Analytical normal-phase TLC was performed on silica gel plates (Silica gel 60 F₂₅₄, 0.25 mm, Merck, Darmstadt, Germany) using a mixture of *n*-hexane-EtOAc (6:4) as eluent. The spots were visualized by exposure to UV radiation (254 nm), or by spraying first with 10% H_2SO_4 in MeOH and then with 5% phosphomolybdic acid in EtOH, followed by heating at 110 °C for 10 min. Low-pressure column chromatography was performed on silica gel columns (Merck, Kieselgel 60, 0.063–0.200 mm). Medium-pressure chromatography was performed with Sepacore system (Büchi, Flawil, Switzerland) on Puriflash prepac normal-phase column (Silica HP, 15 μm , 12G, Interchim, Montluçon, France) using *n*-hexane-EtOAc step gradient elution. Semi-preparative HPLC was carried out with a HPLC system (Breeze, Waters, Milford, MA, USA) equipped with dual-wave UV-vis detector, degasser and column thermostat, on a SymmetryPrep

C18 (7.8 \times 150 mm, 7 μm) column (Waters) using MeCN—0.1% formic acid (6:4) as eluent under the following conditions: detection wavelengths 254 and 280 nm, flow rate 5 ml min⁻¹, temperature 30 °C.

Fungal strain and extraction and purification of chloromonilicin (**1**)

The strain (S-102) of *A. sonchi* used in this study was deposited in the collection of All-Russian Research Institute of Plant Protection (Pushkin, Saint-Petersburg, Russia). The fungus was grown on autoclaved pearl barley and the solid culture was extracted with acetone–water (50:50) according to the procedure previously reported by Evidente *et al.*⁷ After evaporation of the acetone–water phase, the residue was passed through a column containing 20 g of Diaion HP-20 (Sigma-Aldrich, Moscow, Russia), and the column was washed with water, MeOH, EtOAc and CH_2Cl_2 . The dry residue (5.2 g) of the MeOH extract demonstrated both phytotoxic and antimicrobial activity and was fractionated with column chromatography on silica gel with mixtures of CH_2Cl_2 –MeOH (100:0, 95:5, 90:10 and 80:20) to obtain four fractions. The fraction B (3.3 g) showed both phytotoxic and antimicrobial activity and was further separated on silica gel with CH_2Cl_2 –*iso*-PrOH into five fractions. Fraction B2 (80 mg) possessed strong antimicrobial activity. Compound **1** (R_f 0.36 in *n*-hexane–EtOAc 6:4) was purified from this latter fraction by medium-pressure chromatography on silica gel using step gradient of *n*-hexane–EtOAc and finally by semi-preparative HPLC according to the conditions reported above (21 mg; Rt 5.0 min).

Chloromonilicin (**1**)

Melting point 170–171 °C; $[\alpha]_{\text{D}}^{25}$ +202 (c 0.6 CHCl_3); IR ν_{max} : 3481, 1746, 1726, 1646, 1615, 1594 and 1269 cm^{-1} ; UV λ^{MeCN} max nm (ϵ) 279 (18,200) 205 (22,500); CD λ^{MeCN} max nm ($\Delta\epsilon$) 308 (+9.52) 279 (+12.8) 253 (0) 242 (–16.0) 234 (–11.3) 217 (–31.8) 207 (0) 199 (+27.3) (lit. 10: m.p. 169.5–170.5 °C; $[\alpha]_{\text{D}}$ (c 0.4, CHCl_3) +212); UV λ^{MeOH} max nm (ϵ) 276 (20,000); IR ν^{CHCl_3} max cm^{-1} 3040, 1755, 1733, 1655, 1620 and 1602; ^1H and ^{13}C NMR: Table 1; ESI-MS (+) m/z : 723.0232 [calcd for $\text{C}_{32}\text{H}_{22}\text{Cl}_2\text{NaO}_{14}$ 723.0284, $2\text{M}+\text{Na}$]⁺; 388.9805 [calcd for $\text{C}_{16}\text{H}_{11}\text{ClKO}_7$ 388.9830, $\text{M}+\text{K}$]⁺; 373.0065 [calcd for $\text{C}_{16}\text{H}_{11}\text{ClNaO}_7$ 373.0091, $\text{M}+\text{Na}$]⁺.

Crystal structure determination of chloromonilicin (**1**)

Yellow block-shaped single crystals were obtained at ambient temperature by slow evaporation of a C_6H_6 /MeOH (3:1) solution. X-ray data collection was performed at 298 K on a Bruker-Nonius Kappa charge-coupled device diffractometer equipped with graphite-monochromated Mo- $\text{K}\alpha$ radiation ($\lambda = 0.71073$ Å, charge-coupled device rotation images, thick slices, φ and ω scans to fill the asymmetric unit). Cell parameters were obtained from a least-squares fit of the θ angles of 455 reflections in the range $6.663^\circ \leq \theta \leq 16.702^\circ$. A semi-empirical absorption correction (multiscan, SADABS, Bruker, WI, USA) was applied. The structure was solved by direct methods (SIR97 package)¹¹ and refined by the full matrix least-squares method on F^2 against all independent measured reflections (SHELXL program of SHELX97 package).¹² All H atoms were placed in calculated positions and allowed to ride on carrier atoms (C–H in the range 0.95–1.00 Å; $U = 1.2U_{\text{iso}}$ or 1.5 for methyl C) except for the position of the hydroxyl H atom of the two independent molecules found in the asymmetric unit, which was determined from a

difference Fourier map and refined according to a riding model. 22 005 intensities were collected in the range $2.96^\circ \leq \theta \leq 27.02^\circ$, 6302 independent reflections and 443 parameters. Thanks to the presence of the strong anomalous scatterer (chlorine atom), the absolute configuration (S) at C2 atom of both the two independent molecules was established by anomalous dispersion effects obtained in diffraction measurements on the crystal. (Flack's parameter¹³ was 0.06(10) from 3035 Friedel pairs). The final refinement converged to $R_1 = 0.0638$ for 3775 observed reflections having $[I > 2\sigma(I)]$ and $wR_2 = 0.1603$ for all data. Final minimum and maximum residual electronic density was -0.211 and 0.236 e \AA^{-3} . Crystal data: formula $\text{C}_{16}\text{H}_{11}\text{ClO}_7$, formula weight 350.70 g mol^{-1} , hexagonal $P6_5$, $a = 7.9450(5) \text{ \AA}$, $c = 81.655(2) \text{ \AA}$, $\gamma = 120.0^\circ$, $V = 4463.8(4) \text{ \AA}^3$ and $Z = 12$.

CCDC-1031657 contains the supplementary crystallographic data for this paper. These data can be obtained free of charge from The Cambridge Crystallographic Data Centre via www.ccdc.cam.ac.uk/data_request/cif.

Computational section

Merck molecular force field and density functional theory (DFT) calculations were run with Spartan'10 (Wavefunction, Irvine, CA, USA 2010), with standard parameters and convergence criteria. Time-dependent DFT (TDDFT) calculations were run with Gaussian'09 (Gaussian, Wallingford, CT, USA),¹⁴ with default grids and convergence criteria. Conformational searches were run with the Monte Carlo algorithm implemented in Spartan'10 using Merck molecular force field. All structures thus obtained were optimized with DFT method using first B3LYP functional and 6-31G(d) basis set, and then the same functional with 6-311+G(d,p) basis set.¹⁵ The above procedure afforded four minima, of which only the first two had sizable Boltzmann population ($>0.5\%$) at 300 K. TDDFT calculations were run using various functionals (B3LYP, CAM-B3LYP, PBE0, M06) and basis sets (TZVP, aug-TZVP).¹⁵ The CAM-B3LYP/TZVP combination was employed for the final calculations, including 40 excited states (roots), and using the Polarizable Continuum solvent Model in its Integral Equation Formalism (IEF-PCM) for acetonitrile.¹⁵ CD spectra were generated by applying a Gaussian band shape with 0.3 eV exponential half-width, from dipole-length rotational strengths. The difference with dipole-velocity values was checked to be minimal for all relevant transitions.

Biological activities

Antimicrobial activity. The antimicrobial activity of the isolated compounds was tested against a Gram-positive bacterium (*Bacillus subtilis*) and a yeast fungus (*Candida tropicalis*) by using an agar diffusion assay according to the protocol previously described.¹⁶ Both microorganisms were grown on potato-dextrose agar. Up to 100 μg of each metabolite were applied per disc (6 mm in diameter, Macherey-Nagel, Düren, Germany). The cultures were incubated at 30 °C for 24 h before activity was determined by MIC defined as the lowest concentration of antibiotic that inhibited visible growth.¹⁷

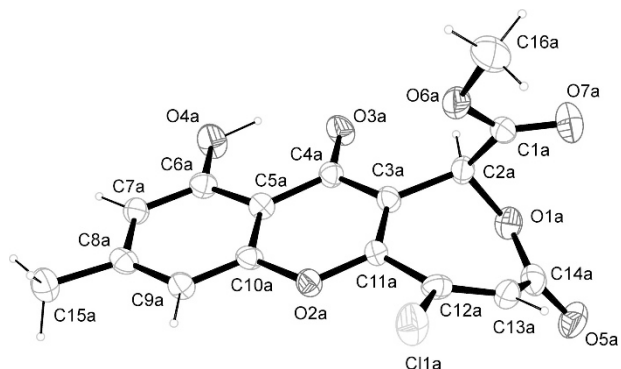


Figure 2 ORTEP view of chloromonilicin (**1**) showing atomic labeling. Displacement ellipsoids are drawn at the 30% probability level. Only one (A) of the two crystallographically independent molecules is shown. A full color version of this figure is available at *The Journal of Antibiotics* journal online.

Antifungal activity. The isolates of plant pathogenic fungi (*A. tenuissima*, *Bipolaris sorokiniana*, *Colletotrichum gloeosporioides* and *Fusarium culmorum*) deposited at the Laboratory of mycology and phytopathology (All-Russian Research Institute of Plant Protection) were grown on potato-dextrose agar under near-UV light or in darkness to produce conidia. The bioassay was performed according to previously described procedures.¹⁸ Fungal conidia were washed out from media with 0.1% solution of Tween-80, adjusted to an appropriate concentration and a suspension (900 μl) was added to the wells of a 24-well plates. Typically the compound **1** (1 mg) was dissolved in EtOH (50 μl) and then water (950 μl) was added. This solution was used for further dilutions in 5% EtOH.

Phytotoxic activity. Leaf segments of *Elytrigia repens* (couch-grass) 2 cm in length and leaf discs of *S. arvensis* (perennial sow thistle) 1 cm in diameter were punctured with a sharp needle in the center and treated with solution of **1** in 5% EtOH at the concentration of 2 mg ml^{-1} as described previously.¹⁹ Typically, for this bioassay samples of **1** (400 μg) were dissolved in EtOH (10 μl) ultrasonically, then water (190 μl) was added and the samples were vortexed. At least 10 replicate leaf segments or discs were used for each treatment.

Zootoxic activity. The antibiotic **1** was evaluated on *Paramecium caudatum* by using the protocol already described by Rao *et al.*²⁰ The assay was performed in a 24-well plate at three different concentrations of chloromonilicin (1, 10 and 100 $\mu\text{g ml}^{-1}$ in 5% EtOH), with three replications for each concentration. The plate was incubated at 24 ± 1 °C. The behavior of the ciliates was observed after 3, 30 and 180 min post treatment using an inverted microscope.

Supporting information

¹H NMR and ¹³C NMR, COSY, HSQC, HMQC, ROESY, IR and HR ESI-MS spectra for chloromonilicin are available as Supplementary Information.

RESULTS AND DISCUSSION

Chloromonilicin (**1**, Figure 1) was originally isolated, together with some related xanthenes such as 4-chloropinselin (**2**, Figure 1), from the cherry rot fungus *Monilinia fructicola*.^{21,22} Chloromonilicin was identified as a growth self-inhibitor with high antifungal activity and a novel structure of a β -chloro- $\alpha,\beta,\gamma,\delta$ -unsaturated ϵ -lactone.^{21,22} Compound **2** appeared a probable biosynthetic precursor of chloromonilicin, while bromomonilicin and bromopinselin were prepared to test biological activity and for biosynthetic studies.²³ Other biosynthetic studies for chloromonilicin were carried out by incorporation of deuterium-labeled synthetic moniliphenone and its xanthone precursor, 4-chloropinselin.²³ The related chloromonilic acids A and B were later isolated from a culture filtrate of *M. fructicola* accumulating chloromonilicin in the mycelium.²⁴

In our work, chloromonilicin (**1**) was purified from the organic extract of the solid culture of *A. sonchi* as reported in detail in the Materials and Methods section. The amorphous yellow solid crystallized slowly from a mixture of benzene–methanol (3:1) giving yellow prisms. It had a molecular formula of $\text{C}_{16}\text{H}_{11}\text{ClO}_7$, as deduced from its HR ESI-MS spectrum. It was identified essentially by ¹H and ¹³C NMR spectra recorded in *d*₆-acetone (data are reported in Table 1). The assignments were supported by the correlations observed in the COSY, HMQC and HMBC spectra,¹⁰ and were consistent with the previously reported spectra recorded in CDCl_3 .²¹ With respect to these latter data (assigned without the support of 2D NMR experiments), we could assign the signal of the phenolic hydroxy group hydrogen-bonded with the O=C-4 as a singlet at δ 11.82 in the ¹H NMR spectrum. Furthermore, the chemical shifts of δ 162.4 and 162.1 were assigned to C-10 and C-11, which previously gave an overlapped signal in the ¹³C NMR spectrum. Their assignments, as well as those of C-5 and C-7, which in CDCl_3 had a very close chemical shift value, were confirmed recording additional spectra in C_6D_6 . In fact, in C_6D_6 they

resonated at δ 155.1, 154.9, 108.2 and 107.6 for C-10, C-11, C-5 and C-7, respectively.

Also the other physical (m.p. and $[\alpha]_D$) and spectroscopic data (UV and IR) were very similar to those previously reported.²¹ Finally, the identification of **1** was supported by the data recorded by HR ESI-MS, which showed the sodiated dimeric form, the potassium and sodium clusters at m/z 723.0232 $[2M+Na]^+$, 388.9805 $[M+K]^+$ and 373.0065 $[M+Na]^+$, respectively.

The identification of chloromonilicin was confirmed by the X-ray analysis of suitable crystals obtained as yellow prisms and the molecular structure is reported in Figure 2. Compound **1** crystallizes in the hexagonal $P6_5$ space group with two independent molecules in the asymmetric unit. The two independent molecules (named A and B) are very similar to each other. Since minimal differences were found in the geometrical parameters, only molecule A is shown in Figure 2.

The molecule skeleton of compound **1** consists of three rings that correspond to a chromen-4-one ring system fused to an oxepin-2(3H)-one ring. All bond lengths and angles are in the normal range and suggest a high degree of conjugation in the molecule. Bond distances and geometry of the two six-membered fused rings confirm the presence of a chromen-4-one moiety that displays an intramolecular OH–O hydrogen bond. The C-3–C-11 and C-12–C-13 bond lengths [1.354(7) and 1.322(8) Å for molecule A; 1.345(7) and 1.319(8) Å for molecule B] confirm the nature of the two C=C double bonds in the seven-membered ring. The molecule of chloromonilicin (**1**) is characterized by a high rigidity. The two six-membered fused rings are planar, while the oxepin-2(3H)-one ring assumes a boat conformation similar to that of 1,3,5-cycloheptatriene,²⁵ with the carboxymethyl group occupying an axial position and H-2 hydrogen

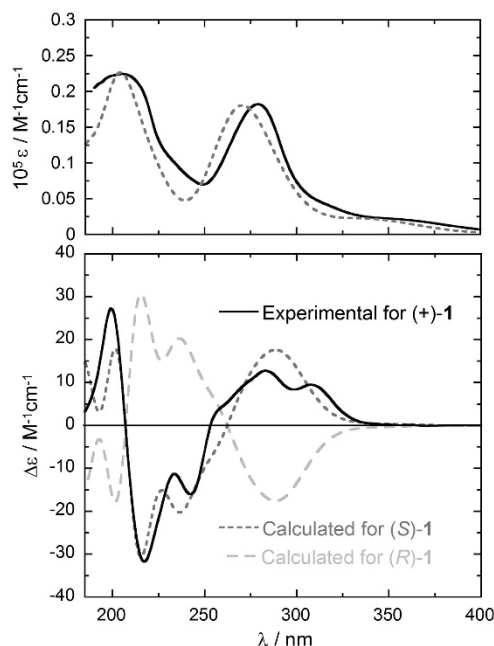


Figure 3 UV–vis absorption (top) and ECD spectra (bottom) of (+)-**1** measured in acetonitrile (solid lines, 4.25 mm, 0.01 cm cell) compared with spectra calculated for (R)-**1** and (S)-**1** with TDDFT at CAM-B3LYP/TZVP//B3LYP/6–311+G(d,p) level as Boltzmann average of two conformers at 300 K (dotted lines). Calculated spectra were obtained as sums of Gaussian bands with 0.3 eV exponential half-width, red-shifted by 18 nm and scaled by a factor 0.5.

an equatorial one. A unique stereogenic center is present in the molecule at C-2 atom. Owing to the strong anomalous scattering of chlorine atoms, it was possible to assign the absolute configuration from X-ray data. In both the two independent molecules the absolute configuration at C-2 was established as (S) by anomalous dispersion effects.

The absolute configuration of (+)-(S)-**1**, established by X-ray analysis, was confirmed by means of ECD spectroscopy. The UV–vis absorption and ECD spectra of (+)-**1** measured in acetonitrile are shown in Figure 3. They feature several bands in the 185–350 nm region, due to the various transitions of the extended conjugated chromophore. The ECD spectrum of (+)-**1** was then calculated with TDDFT²⁶ using the geometries obtained by a consolidated computational procedure.²⁷ This latter consists of a preliminary conformational search with molecular mechanics (Merck molecular force field) using a Monte Carlo algorithm, followed by DFT geometry optimizations; the details are described in the Computational section. As a result, only two low-energy conformers populated at 300 K were obtained for chloromonilicin, because of the relatively rigid cyclic skeleton. The lowest-energy conformer found by B3LYP/6–311+G(d,p) optimizations, depicted in Figure 4, accounts for 70% population at 300 K and it is almost coincident with the X-ray structure (the root-mean square deviation between the two structures for non-hydrogen atoms is 0.23 Å). The second conformer (relative energy +0.50 kcal mol⁻¹,

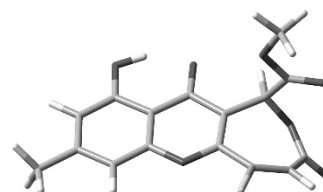


Figure 4 Lowest-energy B3LYP/6–311+G(d,p) structure of (S)-**1**. A full color version of this figure is available at *The Journal of Antibiotics* journal online.

Table 2 Effect of the concentration of chloromonilicin on growth inhibition (zone of lysis, mm) of five microorganisms

Microorganism	μg Per disc			
	0.5	1.0	2.5	5.0
<i>Escherichia coli</i>	3±0	4.5±0.5	5.5±0.5	6±0
<i>Pseudomonas fluorescens</i>	4.5±0.5	5.5±0.5	7±0	7.5±0.5
<i>Bacillus subtilis</i>	7±0	9.5±0.5	11±0	12.5±0.5
<i>Paenibacillus polymyxa</i>	0	1±0	2±0	2±0
<i>Candida tropicalis</i>	0.5±0.5	1.5±0.5	3±0	4±0

Table 3 Effect of the concentration of chloromonilicin on percentage of germinated conidia of four phytopathogenic fungi

Fungal specie	$\mu g ml^{-1}$			
	0	1	10	100
<i>Fusarium culmorum</i>	100±0	58.7±12.5	0	0
<i>Bipolaris sorokiniana</i>	87.5±3.5	55.1±12.9	0	0
<i>Colletotrichum gloeosporioides</i>	67.3±2.2	0	0	0
<i>Alternaria tenuissima</i>	91.9±1.5	79.1±2.4	12.1±1.9	4.7±0.4

30% population) differs from the absolute minimum only in the rotamerism around the C-1–C-2 bond. The axial arrangement of the carboxymethyl group minimizes the electrostatic repulsion between the carboxymethyl and ketone moieties. ECD spectra were calculated on the two conformers with TDDFT method using various combinations of functionals and basis sets (see Computational section). In all cases, the spectra calculated for the two conformers were very similar. The Boltzmann-weighted spectra computed for both enantiomers of **1** at CAM-B3LYP/TZVP level of theory, and including a solvent model for acetonitrile, are shown in Figure 3. The good agreement observed between the calculated spectrum for (S)-**1** and the experimental spectrum allowed us to definitely establish the absolute configuration of chloromonilicin as (+)-(S)-**1**.

Chloromonilicin showed a wide spectrum of antimicrobial activity against bacteria, yeast and plant pathogenic fungi. When the compound was assayed by paper disc technique, the MIC against *Ba. subtilis*, *Escherichia coli* and *Pseudomonas fluorescens* was lower than 0.5 µg per disc (Table 2). Other two microorganisms tested (*Paenibacillus polymyxa* and *Ca. tropicalis*) were less sensitive to chloromonilicin with MIC about 1 µg per disc (Table 2). Chloromonilicin demonstrated ability to inhibit germination of conidia of four widely distributed plant pathogenic fungi, namely, *A. tenuissima*, *Bi. sorokiniana*, *Co. gloeosporioides* and *F. culmorum*, with MIC < 1 µg ml⁻¹ (Table 3).

Chloromonilicin was tested for its phytotoxic activity on punctured leaf discs of perennial sow thistle and leaf segments of couch-grass and no activity of this compound was found even at the highest concentration of 2 mg ml⁻¹ used in this study.

At the minimal concentration of 1 µg ml⁻¹ the antibiotic **1** fully inhibited the movement of *Par. caudatum* after 1 h post treatment. At the higher concentrations of chloromonilicin (10 and 100 µg ml⁻¹) the ciliates were dead after 20 and 10 min of incubation, respectively. So, although the antibiotic did not demonstrate acute toxicity, at the lowest concentration it remained still active against *Par. caudatum*.

In an earlier study of Sassa *et al.*,²¹ where they used agar dilution method on glucose nutrient agar, chloromonilicin showed marked antifungal activity against the human pathogenic fungi *Candida albicans* and *Trichophyton* spp. (1.5–6.2 µg ml⁻¹), while a number of tested bacteria were almost insensitive to the antibiotic (MIC ≥ 50 µg ml⁻¹). Chloromonilicin possessed also hyphal growth-inhibiting activity against its producing fungus, *M. fructicola* at 5 µg per disc.²¹ The differences in the results on the antibacterial activity of **1** in the above mentioned study and in our research can be explained with the different bioassays techniques used as well as the different sensitivity of bacteria to this antibiotic.

In this study, we also demonstrated the absence of phytotoxic activity of chloromonilicin on leaves of two plants and high activity against some plant pathogenic fungi. Possibly, this metabolite is a defense factor of *A. sonchi* against antagonistic microorganisms. From a practical point of view chloromonilicin can potentially be used as a natural non-phytotoxic fungicide to protect crops from fungal diseases. However, toxicological studies of chloromonilicin as well as its producing organism are necessary because of the toxic effect of this compound on *Par. caudatum*. Future studies are needed to enlarge the production of the antibiotic and evaluate its *in vivo* conditions. The former step might be reached by media and strain selection, optimization of culture conditions and of compound isolation and purification processes.

In conclusion, chloromonilicin was isolated for the first time as the main antimicrobial metabolite produced by *A. sonchi*. This was the occasion to assign its absolute configuration, not reported before, and

to extensively investigate its biological activity. The results obtained pushed us to plan a scale-up production of this promising antimicrobial metabolite to test it in *in vivo* experiments. However, additional toxicology studies should be carried out to confirm the potential of chloromonilicin for practical application as antimicrobial agent in agriculture and/or medicine.

ACKNOWLEDGEMENTS

We thank Mr L Chisty and Dr V Zakharov (Research Institute of Hygiene, Occupational Pathology and Human Ecology, Federal Medical Biological Agency, St Petersburg, Russian Federation) for NMR and Dr A Rudenko (Institute of Toxicology, Federal Medical Biology Agency, Saint-Petersburg, Russian Federation) for HR ESIMS spectra. The research work of the Russian group on production, isolation and biological characterization of bioactive metabolites produced by plant pathogens was supported by Russian Fund of Basic Research (project N 12-04-00853). This research was carried out in part in the frame of Programme STAR, financially supported by UniNA and Compagnia di San Paolo. AE is associated with the Istituto di Chimica Biomolecolare del CNR, Pozzuoli, Italy.

- 1 Donald, W. W. Management and control of Canada thistle (*Cirsium arvense*). *Rev. Weed Sci.* **5**, 193–250 (1990).
- 2 Evans, H. C. in *Biological Control of Weeds with Fungi. The Mycota*, Vol. 11, 145–172 (Springer-Verlag, Berlin Heidelberg, 2013).
- 3 Cimmino, A. *et al. Abstracts of Papers 8th PSE (The Phytochemical Society of Europe) Meeting on Biopesticides*, La Palma, Canary Islands, Spain, 2009.
- 4 Vurro, M. in *Novel Biotechnologies for Biocontrol Agent Enhancement and Management* (eds Vurro, M. & Gressel, J.), Ch. 3, 53–74 (Springer, Netherlands, 2007).
- 5 Cimmino, A., Andolfi, A., Berestetskiy, A. & Evidente, A. Production of phytotoxins by *Phoma exigua* var. *exigua*, a potential mycoherbicide against perennial thistles. *J. Agric. Food Chem.* **56**, 6304–6309 (2008).
- 6 Berestetskiy, A. O. & Kurlenya, A. S. Antimicrobial properties of some phytopathogenic micromycetes. *Mikologia Fitopatologia* **48**, 123–134 (2014).
- 7 Evidente, A., Punzo, B., Andolfi, A., Berestetskiy, A. & Motta, A. Alternethanoxin A and B, polycyclic ethanones produced by *Alternaria sonchi*, potential mycoherbicides for *Sonchus arvensis* biocontrol. *J. Agric. Food Chem.* **57**, 6656–6660 (2009).
- 8 Berestetskiy, A. *et al.* Alternethanoxins C-E, further polycyclic ethanones produced by *Alternaria sonchi*, a potential mycoherbicide for *Sonchus arvensis* biocontrol. *J. Agric. Food Chem.* **63**, 1196–1199 (2015).
- 9 Bury, M. *et al.* Evaluation of the anticancer activities of two fungal polycyclic ethanones, alternethanoxins A and B, and two of their derivatives. *Int. J. Oncol.* **38**, 227–232 (2011).
- 10 Berger, S. & Braun, S. *200 and More Basic NMR Experiments: A Practical Course* (Wiley-VCH, Weinheim, 2004).
- 11 Altomare, A. *et al.* A new tool for crystal structure determination and refinement. *J. Appl. Crystallography* **32**, 115–119 (1999).
- 12 Sheldrick, G. M. A short history of SHELX. *Acta Crystallogr.* **A64**, 112–122 (2008).
- 13 Flack, H. D. On enantiomorph-polarity estimation. *Acta Crystallogr.* **A39**, 876–881 (1983).
- 14 Frisch, M. J. *et al. Gaussian'09, Revision D.01*, (Gaussian, Inc., Wallingford, CT, 2013).
- 15 All references about DFT functionals, basis sets and solvent models can be found in the on-line documentation for Gaussian'09 at www.gaussian.com/g_tech/g_url/g09help.htm.
- 16 Bottalico, A., Capasso, R., Evidente, A., Randazzo, G. & Vurro, M. Cytochalasins: structure-activity relationships. *Phytochemistry* **29**, 93–96 (1990).
- 17 Onishi, H. R. *et al.* Antibacterial agents that inhibit lipid A biosynthesis. *Science* **274**, 980–982 (1996).
- 18 Talontsi, F. M. *et al.* Zoosporicidal metabolites from an endophytic fungus *Cryptosporiopsis* sp. of *Zanthoxylum lepreurii*. *Phytochemistry* **83**, 87–94 (2012).
- 19 Berestetskiy, A. O. *et al.* Isolation, identification, and characteristics of the phytotoxin produced by the fungus *Alternaria cirsinioxia*. *App. Biochem. Microbiol.* **46**, 75–79 (2010).
- 20 Rao, J. V., Srikanth, K., Arepalli, S. K. & Gunda, V. G. Toxic effects of acephate on *Paramecium caudatum* with special emphasis on morphology, behaviour, and generation time. *Pestic. Biochem. Phys.* **86**, 131–137 (2006).
- 21 Sassa, T., Kachi, H. & Nukina, M. Chloromonilicin, a new antifungal metabolite produced by *Monilinia fructicola*. *J. Antibiot. (Tokyo)* **38**, 439–441 (1985).
- 22 Kachi, H., Hattori, H. & Sassa, T. A new antifungal substance, bromomonilicin, and its precursor produced by *Monilinia fructicola*. *J. Antibiot. (Tokyo)* **39**, 164–166 (1986).
- 23 Kachi, H. & Sassa, T. Isolation of moniliphenone, a key intermediate in xanthone biosynthesis from *Monilinia fructicola*. *Agric. Biol. Chem.* **50**, 1669–1671 (1986).

- 24 Sassa, T., Horiguchi, K. & Suzuki, Y. Chloromonilinic acids A and B, novel catabolites of the growth self-inhibitor chloromonilicin isolated from *Monilinia fructicola*. *Agric. Biol Chem.* **53**, 1337–1341 (1989).
- 25 Traetteberger, M. The molecular structure of 1,3,5-cycloheptatriene in the vapor phase as determined by the sector electron diffraction method. *J. Am. Chem. Soc.* **86**, 4265–4270.
- 26 Autschbach, J. Computing chiroptical properties with first-principles theoretical methods: Background and illustrative examples. *Chirality* **21**, E116–E152 (2009).
- 27 Pescitelli, G., Di Bari, L. & Berova, N. Conformational aspects in the studies of organic compounds by electronic circular dichroism. *Chem. Soc. Rev.* **40**, 4603–4625 (2011).

Supplementary Information accompanies the paper on The Journal of Antibiotics website (<http://www.nature.com/ja>)